Chapter 9

Preparation, Characterization and Applicability of Covalently Functionalized MWNT

Eun-Soo Park

Additional information is available at the end of the chapter

http://dx.doi.org/10.5772/50883

1. Introduction

Over the last twenty years, carbon nanotubes (CNTs) have received much attention for their unique structural, mechanical, and electronic properties as well as their broad range of potential applications [Lee et. al., 2012; Kim and Park, 2008; Kang et. al., 2008; Xu et. al., 2008; Meyyappan et al., 2005; Kumar, 2002; Wong et al., 1998]. CNTs are cylinder-shaped macromolecules with a radius as small as a few nanometers, which can be grown up to 20 cm in length [Zhu et. al., 2002]. Their properties depend on the atomic arrangement, chirality, diameter, and length of the tube and the overall morphology. They exist in one of two structural forms, single-walled CNT (SWNT) or multi-walled CNT (MWNT). SWNTs are best described as a 2-D graphene sheet rolled into a tube with pentagonal rings as end caps [Harris, 2004]. SWNTs have aspect ratios of 1000 or more and an approximate diameter of 1 nm. Similarly, MWNTs can be described as multiple layers of concentric graphene cylinders also with pentagonal ring end caps. Conventional MWNT diameters range from 2-50 microns [Harris, 2004]. Measurements using in situ transmission electron microscopy (TEM) and atomic force microscopy (AFM) have produced estimates that Young's modulus of CNTs is approximately 1 TPa [Treacy et. al., 1996; Wong et. al., 1997]. For comparison, the stiffest conventional glass fibers have Young's modulus of approximately 70 GPa, while carbon fibers typically have modulus of about 800 GPa. CNTs can accommodate extreme deformations without fracturing and also have the extraordinary capability of returning to their original, straight, structure following deformation [Harris, 2004]. In addition, they are excellent electrical conductors and have very high thermal conductivities. Possible applications for CNTs range from nanoelectronics, quantum wire interconnects, sensors and field emitters to nanocomposites [Meyyappan et. al., 2005].

Despite these great promises, many real applications of CNTs have been impeded by difficulties associated with their processing and manipulation. As produced CNTs have the tendency to exist in bundles rather than as individual tubes, because of strong van der Waals interactions, leading to insolubility in most organic media, and therefore limiting the range of applications [Neelgund and Oki, 2011]. To make CNTs more easily dispersible in various media, it is necessary to physically or chemically attach certain molecules, or functional groups, to their smooth sidewalls without significantly changing the CNTs desirable properties. This process is called functionalization. Various functionalization methods such as chopping, oxidation, wrapping and irradiation of the CNTs can be created more active bonding sites on the surface of the nanotubes. Among them, electron beam (EB) irradiation is potent to induce the uniform and consistent modification of the nanotubes because of the high amount of energy, it imparts to the atoms via the primary knock-on atom mechanism. This chapter describes a novel method to covalently functionalized nanotubes that bear terminated isocyanate, hydroxyl, amine and epoxy group, which then react covalently with other molecules. The first step is preparation of COOH-terminated MWNT by EB irradiation of unmodified nanotubes. These carboxylic groups were used as reaction precursors in the covalent functionalization. The MWNTs attached to the organofunctional moieties have greater versatility for further utilization in different application fields such as macroinitiator, electroconductive nanocomposite, biology, water treatment, and starting material for another cycle of functionalization. Moreover covalently functionalized nanotubes can extend the field of application in nanoelectronics, sensorics, hydrogen power engineering, bioengineering, and medicine [Dresselhaus and Dresselhaus, 2001; Burghard, 2005].

2. Preparation and characterization of covalently functionalized MWNT

The non-reactive nature of the CNT surface appears as a constraint in several technological applications. To manipulate and process CNTs, it is desirable to functionalize the sidewall of CNTs, thereby generating CNT-derivatives that are compatible with solvent as well as organic matrix materials. Modification of the CNT surface by changing its chemical composition has proved to be efficient to overcome this problem. Several methods such as chemical functionalization, non-covalent wrapping and high energy beam irradiation have been used to modify the chemical composition of the CNT surface by grafting functional groups to it.

Chemical functionalization of CNT has been performed mainly on the basis of oxidative treatments [Abuilaiwi et. al., 2010; Basiuk et. al., 2004; Lee et. al. 2005; Balasubramanian and Burghard, 2004]. Typically this is achieved by the oxidative process of CNTs using strong inorganic acids or oxidizing agents. This is a lengthy process that also generates a lot of waste and that can damage the CNT structure. Moreover these conventional surface treatment methods utilize a reaction between a liquid and a solid since an oxidizing agent contacts with the entire surface of CNT and the surface is uniformly reacted or physically treated, it is difficult to control the surface state.

The non-covalent method to functionalize CNTs involves using surfactants, oligomers, biomolecules, and polymers to wrap CNTs to enhance their solubility [Hirsch, 2002]. Using pol-

http://dx.doi.org/10.5772/50883

ymer chains to wrap CNTs is a versatile and effective way for CNT functionalization. Block copolymers may provide a series of attractive non-covalent wrapping and decoration for the functionalization of CNTs [Chen et. al., 2011]. These approaches can be driven by distinct interactions between nanotubes and polymers including p-stacking, electrostatic interactions, and decoration of CNTs with micelles [Zou et. al., 2008]. One block of the block copolymers forms a close interaction with CNTs, while the other block provide the dispersibility and chemical compatibility to the CNTs [Szleifer and Yerushalmi-Rozen, 2005]. However, the non-covalent interaction between the wrapping molecules and the CNTs is not as strong as the covalent bonding formed in the chemical functionalization methods [Hirsch, 2002].

Electron and ion irradiation is generally used nowadays for modifying properties of semiconductors; beams of energetic particles are also expected to be widely employed for nanotube-based materials processing [Krasheninnikov and Nordlund, 2004]. EB irradiation is a form of ionizing energy that is generally characterized by its low penetration and high dosage rates. The beam with a concentrated and highly charged stream of electrons is generated by the acceleration and conversion of electricity. The electrons are generated by equipment referred to as accelerators which are capable of producing beams that are either pulsed or continuous. When an electron hits the target, different mechanisms of damage creation can work. Depending on the target material, the main mechanism can be the kinetic energy transfer, electronic excitations and ionization [Krasheninnikov and Nordlund, 2004]. For CNTs, the most important mechanism is the knock-on atom displacements due to kinetic energy transfer for electrons [Dresselhaus and Avouris, 2001]. Electronic excitations and ionization effects seem to be less important due to a high thermal and electrical conductivity of graphene shells [Banhar, 1999].

2.1. Functionalization of MWNT by electron-beam irradiation

The MWNT (purity = 95 wt %, average diameter = 15 nm, average length = 20 μm, specific gravity = 1.8) was received from the Iljin Nanotech Co., Ltd., Korea. Fig. 1 shows the TEM image and energy-dispersive X-ray spectroscope analysis (EDX) result of MWNT produced by a chemical vapour deposition (CVD) process without any purification. The TEM measurements were performed with a Philips CM200 operated at 200 kV. Scanning electron microscopy (SEM) observations of the MWNT samples were performed on a Hitachi model S-4300, Japan. The morphology was determined at an accelerating voltage of 15 kV. The surface sample composition was evaluated with SEM equipped with an EDX spectroscope.

As-received MWNT contain some impurities and entangle into a bulk piece (Fig. 1a). EDX results of the pristine MWNT show small peaks which are corresponding to Fe, Si and S. The Si peak has its origin in silicon substrate whereas the other peaks are due to the precursor gases present in the gas mixture and catalyst. The Pt peaks was due to the platinum sputtering process during sample preparation. CNTs are often formed in entangled ropes with 10–100 CNTs per bundle depending on the method of synthesis. They can be produced by a number of methods: direct-current arc discharge, laser ablation, thermal and plasma

enhanced CVD process [Lau and Hui, 2002]. The method of production affects the level of purity of the sample and whether SWNTs or MWNTs are formed. Impurities exist as catalysis particles, amorphous carbons and non-tubular fullerenes [Thostenson et. al., 2001].

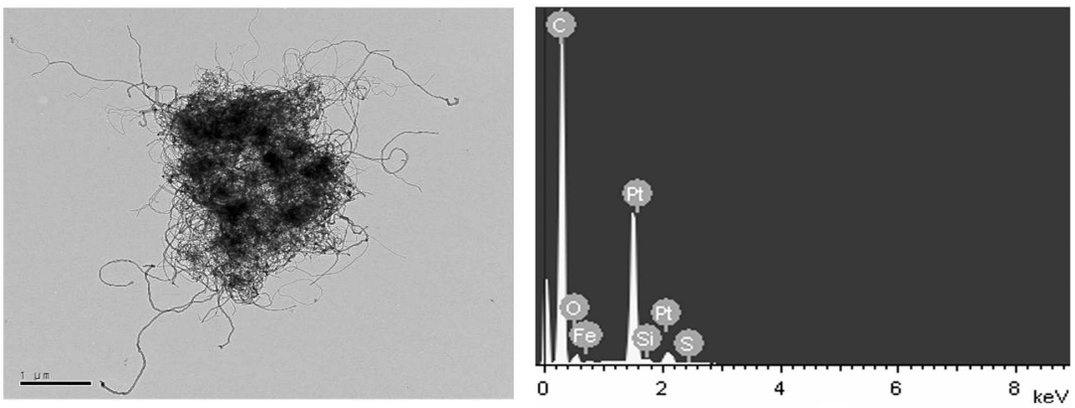

Figure 1. TEM image (a) and EDX analysis (b) result of the pristine MWNT.

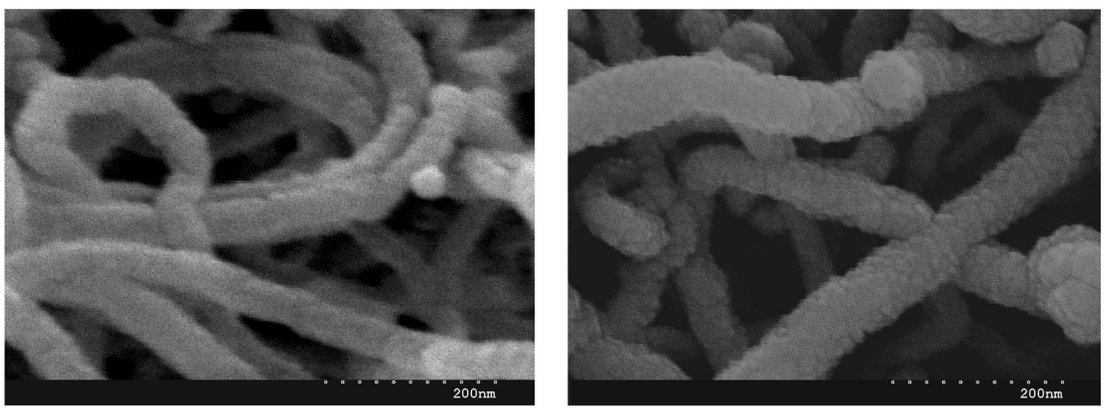

Figure 2. SEM image of the MWNT before (a) and after (b) EB irradiation at 1200 kGy.

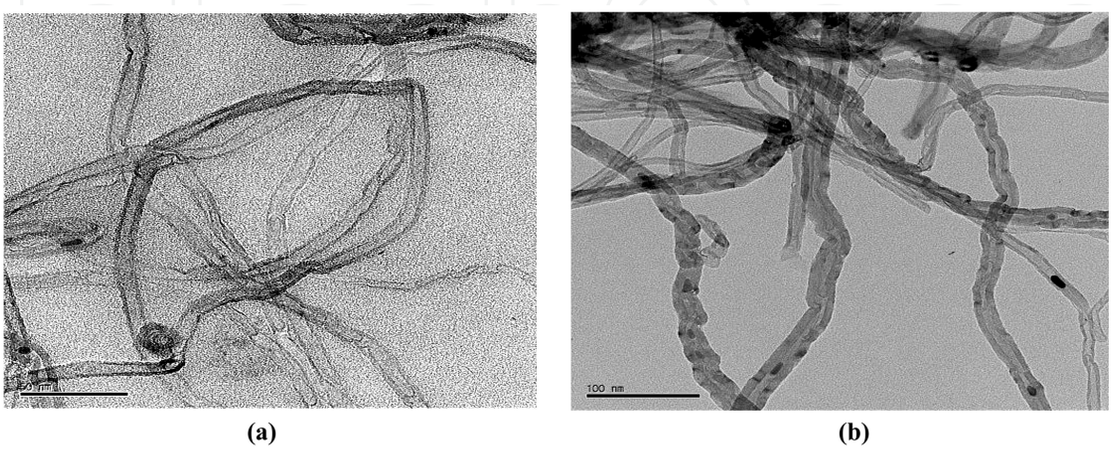

Figure 3. TEM image of the MWNT before (a) and after (b) EB irradiation at 1200 kGy.

http://dx.doi.org/10.5772/50883

The MWNT were EB-irradiated in air at room temperature using a 1.5MeV electrostatic accelerator (ELV-4, EB Tech Co., Ltd., Korea). Irradiation dose of 800, 1000, and 1200 kGy were used, respectively. The specifications of the ELV-4 are presented Table 1.

Model	Energy (MeV)	Maximum Current (mA)	Output (kW)	Window length (mm)	Height (mm)
ELV-4	0.8 ~ 1.5	50	50	980	4330

Table 1. Specifications of the ELV-4 EB accelerator.

Fig. 2 demonstrates higher magnification SEM micrographs of MWNT before and after treatment with the EB irradiation. The pristine MWNT has relatively smooth surface without extra phase or stain attached on its sidewall. Although the EB irradiation increased up to 1000 kGy, the surface appearance little changed compare to the pristine MWNT. After the 1200 kGy EB irradiation, the smooth surface was disappeared, many wrinkled structure were formed, and the surface roughness increased. Additional sample characterization is carried out using TEM. From the Fig. 3, the presence of dark spots on the outer wall of the MWNT1200 suggests that damage and formation change of MWNT induced by high-dose irradiation.

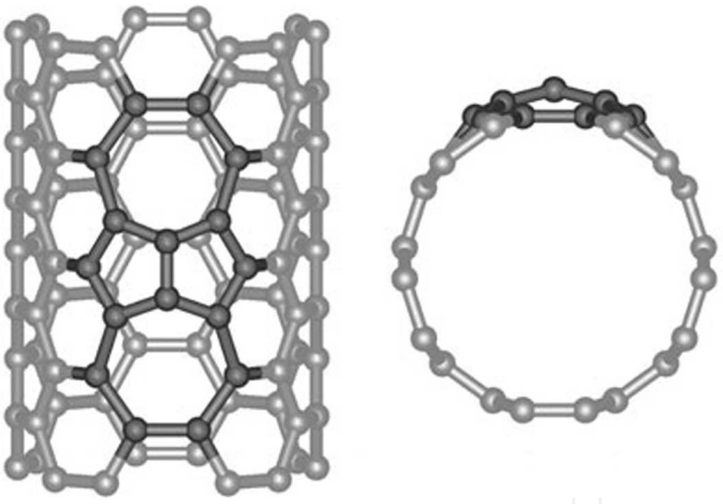

Figure 4. Stone–Wales defect on the sidewall of a nanotube [Burghard and Balasubramanian, 2005].

In general, the surface of the synthesized CNT is smooth and relatively defects free. However, stresses can induce Stone-Wales transformations, resulting in the formation of heptagons and concave areas of deformation on the nanotubes [Thostenson et. al., 2001; Burghard and Balasubramanian, 2005]. Moreover EB irradiation of MWNTs resulted in forming vacancies on their walls and eventual amorphization upon high-dose irradiation [Banhart, 1999]. The irradiation induced damage manifested itself in the deterioration of mechanical properties of MWNTs exposed to prolonged 2-MeV electron irradiation [Salvetat et. al., 1999].

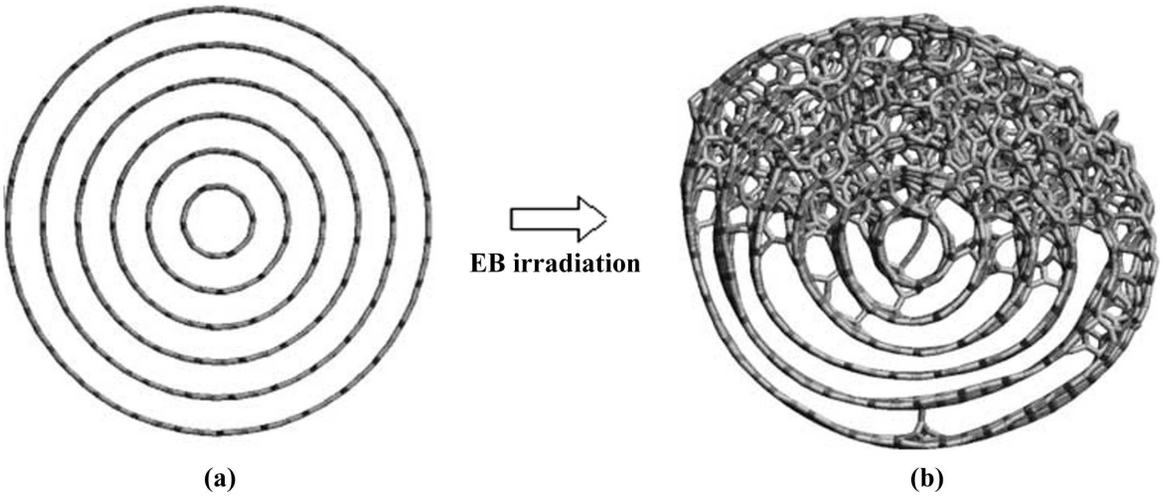

Figure 5. Molecular model of MWNT before (a) and after (b) 300-eV Ar ion irradiation with a dose of $2\times10^{16}/cm^2$ [Krasheninnikov and Nordlund, 2004].

2.2. Characterization of EB-MWNT

The pristine MWNT and EB-irradiated MWNT were characterized by Fourier transform infrared (FTIR) spectroscopy. FTIR spectra of the KBr pelleted samples were measured with a PerkinElmer infrared spectrometer (Spectrum 2000) in the wave-number range from 4000 to 400 cm^{-1} and were analyzed with commercial software.

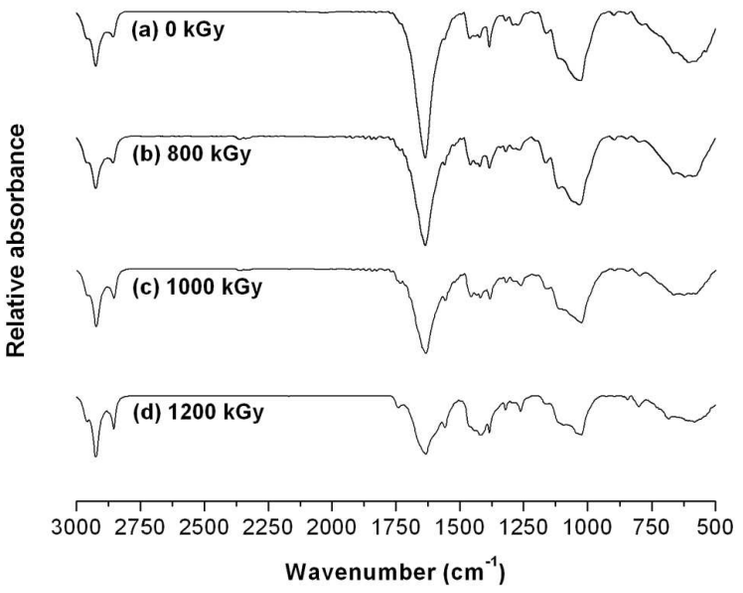

Figure 6. FTIR spectra of the EB-irradiated MWNT.

http://dx.doi.org/10.5772/50883

From Fig. 6, the strong bands at 2920 and 2852 cm^{-1} on the curve are well known, due to asymmetrical and symmetrical stretching of -CH_2, respectively. The band at 2958 cm^{-1} is assigned to the asymmetrical stretching of -CH_3. The peak at 1635 cm^{-1} can be associated with the stretching of the MWNT backbone. FTIR spectra of MWNT after EB irradiation more than 1000 kGy showed new peaks at 1782-1720 cm^{-1} due to the C=O bond resulting from the stretch mode of carboxylic groups (Fig. 6). These groups can then be used to link molecules via covalent bond formation.

EDX results also confirmed that the oxygen content in the MWNTs increased significantly after irradiation at 1000 kGy. The abbreviation of the sample code in Table 2, MWNT800, for example, means that the MWNT was EB-irradiated at radiation dose of 800 kGy. Oxygen atom on the surfaces of pristine MWNT may be due to the partial oxidation of the surfaces of MWNTs during manufacturing or purification by the manufacturer.

Element	Composition (atomic%)			
	MWNT	MWNT800	MWNT1000	MWNT1200
C	94.63	91.25	88.32	83.47
O	5.11	7.62	9.81	15.32
Si	0.14	1.05	1.70	1.21
S	0.03	-	-	-
Fe	0.09	0.08	0.17	-

Table 2. EDX analysis result of the pristine MWNT and EB-MWNT.

Elemental analyses (EA) results of the MWNT and EB-MWNT are shown in Table 3. EA was performed in a Thermo EA1112 apparatus. The results presented a decrease in the hydrogen content up to 1000 kGy. After the 1200 kGy irradiation, the hydrogen content was significantly increased. This indicated that the low irradiation dose cleaned the MWNT surface of impurities, according to the SEM, EDX and EA results, but the increase in the irradiation doses could have affected the surface roughness and chemical composition [Lee et. al., 2012].

Element	Composition (%)			
	MWNT	MWNT800	MWNT1000	MWNT1200
C	99.50	99.52	99.52	99.35
H	0.50	0.48	0.48	0.57
N	-	-	-	0.08

Table 3. EA results of the pristine MWNT and EB-MWNT.

2.3. Properties of EB-MWNT

2.3.1. Thermal stability

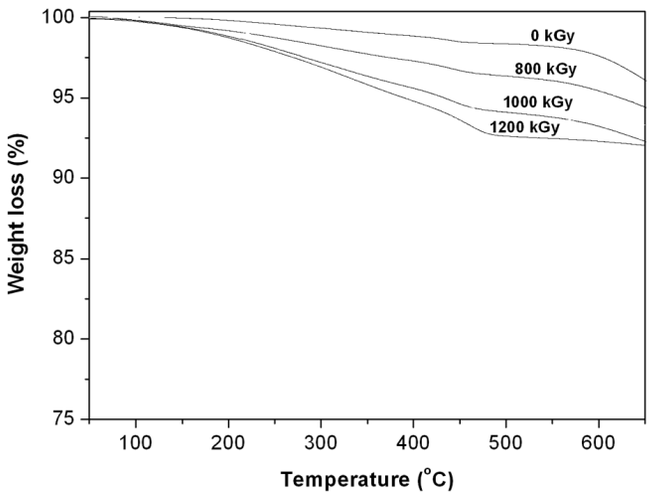

Figure 7. TGA thermograms of the pristine MWNT and EB–MWNTs (Lee et. al., 2012).

Fig. 7 provides quantitative information on the EB-MWNT by using thermogravimetry (TGA, PerkinElmer TGS-2) results. The TGA curves were obtained under an N_2 atmosphere and scanned from 20 to 800°C at a heating rate of 20°C/min. As shown in Fig. 7, the pristine MWNT did not show any discernible thermal degradation, with only 2 wt% degradation at 600°C. On the contrary, the weight loss of the EB–MWNTs significantly increased with increasing irradiation dose because of the possible destruction of the CNT structure. The damage formation in CNTs is quite different from that observed in most other solids [Krasheninnikov and Nordlund, 2004]. Nitric acid or other oxidizing media, such as ozone or oxygen plasma, have been reported to be effective for the partial surface oxidation of CNTs [Banerjee et. al., 2005]. It has been shown that the basal planes of graphite are attacked by molecular oxygen only at their periphery or at defect sites, such as edge planes and vacancies [Radovic, 2003]. Along with the simple defects, a number of more complex defects can be formed such like the Stone–Wales defects [Burghard and Balasubramanian, 2005] associated with a rotation of a bond in the CNT atom network, other topological defects in the graphitic network, and amorphous complexes. Besides this, defect-mediated covalent bonds between adjacent SWNTs in the bundle can appear. Likewise, similar links between shells can appear in MWNTs [Krasheninnikov and Nordlund, 2004].

2.3.2. Electrical resistivity

Table 4 shows a rapid decrease in volume resistivity of the poly(ethylene-*co*-vinyl acetate (EVA, vinyl acetate content = 28%)/EB–MWNT nanocomposites with increasing nanotube content. The surface electrical resistance of specimens (80 mm × 10 mm) was detected by a

http://dx.doi.org/10.5772/50883

megohmmeter (TeraOhm 5 kV, Metrel) according to ASTM D 257. The charge time was 30 s, and the current stress of the measurements was 2500 V at 20 ± 1°C. Volume resitivity values of the prepared films were calculated with the following equation:

$$\varrho_v = \frac{AR_v}{L} \tag{1}$$

Where ρ_v, A, R_v and L represent the area of the volume resistivity (Ω-cm), effective electrode (cm^2), measured resistance (Ω), and distance between electrodes (cm), respectively.

The percolation threshold of the EVA/MWNT nanocomposites formed by solution mixing was approximately ~ 5 wt %; this was due to the advantageous effect of composites with higher aspect ratios compared with spherical or elliptical fillers in the formation of conducting networks in the polymer matrix [Lee et. al., 2012]. However, volume resistivity of nanocomposites was not significantly changed with irradiation dose indicated that EB irradiation did not affect the electroconductivity of MWNT.

Nanotube content (wt%)	Volume resistivity (Ω-cm × 10^{-5})			
	MWNT	MWNT800	MWNT1000	MWNT1200
0.0	474,600	474,600	474,600	474,600
2.5	107,083	104,900	100,983	100,271
5.0	2.48	2.46	2.10	2.10
10	0.015	0.015	0.014	0.014

Table 4. Volume resistivity changes of the EVA/EB-MWNT nanocomposites (Lee et. al., 2012).

2.3.3. Biological activity

The biological activity of the pristine MWNT and EB-MWNT was compared against *Staphylococcus aureus* (*S. aureus*, ATCC 25923) and *Escherichia coli* (*E. coli*, ATCC 25922) with the shake flask method. The bacteria cell were subcultured on nutrient broth and incubated for 20 h at 37°C. The cells were suspended in 50 ml of phosphate-buffered saline (PBS) to yield a bacterial suspension of 2.32×10^9 – 2.49×10^9 colony forming units/ml (cfu/ml). The nanotube (0.5 g) was weighed and shaken in 20 ml of a bacterial suspension for 24 h. The suspension (25 wt/vol%) was serially diluted in PBS and cultured on nutrient broth at 37°C for 24 h. The number of viable organisms in the suspension was determined by multiplication of the number of colonies with the dilution factor, and the percentage reduction was calculated on the basis of the initial count. *S. aureus* and *E. coli* are two of the most common nosocomial pathogens and they represent Gram-positive and Gram-negative bacteria, respectively. The number of viable bacteria and the percentage reduction of the number of bacteria are summarized in Table 5.

Sample	Antibacterial activity			
	S. aureus (+)		*E. coil (-)*	
	cfu/ml ($\times 10^{-9}$)	Reduction (%)	cfu/ml ($\times 10^{-9}$)	Reduction (%)
Blank	2.32	-	2.49	-
MWNT	2.13	8.2	2.08	10.3
MWNT800	1.85	20.3	1.93	16.8
MWNT1000	1.72	25.9	1.78	23.3
MWNT1200	1.65	28.9	1.55	33.2

Table 5. Shake flask test results for the pristine MWNT and EB-MWNT.

After 24 h of bacterial contact, pristine MWNT extirpated 8.2 and 10.3 % of the viable cells of *S. aureus* and *E. coil*, respectively. This indicated that pristine MWNT has some interesting biological activities. Harmful effect of nanoparticles arises due to high surface area and intrinsic toxicity of the surface. The nano-scale dimensions of CNT make quantities of milligrams possess a large number of cylindrical particles with a concurrent very high total surface area. The intrinsic toxicity of CNT depends on the degree of surface functionalization and the different toxicity of functional groups. Batches of pristine CNT readily after synthesis contain impurities such as amorphous carbon and metallic catalysts which can also be the source of toxic effects [Singh et. al., 2010]. Kang and co-workers [Kang et. al., 2008] showed that the size of CNTs is a key factor governing their antibacterial effects and that the likely main CNT-cytotoxicity mechanism is cell membrane damage by direct contact with CNTs. As the size of CNTs decreases, the specific surface area increases, leading to increased opportunity for interaction and uptake by living cells. This characteristic could result in adverse biological effects that otherwise would not be possible with the same material in a larger form [Donaldson et. al., 2004; Nel et. al., 2006; Jia et. al., 2005]. Several studies have shown that SWNTs exhibit significant cytotoxicity to human and animal cells, whereas MWNTs exhibit a milder toxicity [Jia et. al., 2005].

With the EB irradiation dose the biological activity of MWNT against both the *S. aureus* and *E. coil* was gradually increased. It is noteworthy that 1200 kGy irradiated MWNT exhibits highest antibacterial activity against *S. aureus*. After 24h of shaking, MWNT1200 showed 33.2 % inhibition of the growth of *S. aureus*. In order to inactivate or kill microbes, the nanocomposite particles must come close to or touch the microbes. Such interactions are either attraction or repulsion. As most bacteria carry a net negative surface charge [Jucker et. al., 1996], adhesion of bacteria is discouraged on negatively charged surfaces, while it is promoted on positively charged surfaces [Hogt et. al., 1986]. The increase in polarity of MWNT after EB irradiation is reflected in the relative polar surface area, hydrogen bond donor, and hydrogen bond acceptor numbers, all of which increase substantially for biological activity [Lee et. al., 2011].

http://dx.doi.org/10.5772/50883

2.4. Covalent functionalization of EB-MWNT

The sites of highest chemical reactivity within CNTs are the caps, which have a fullerene like structure [Balasubramanian and Burghard, 2008]. CNTs are not ideal structures, but rather contain defects formed during synthesis. Typically around 1–3 % of the carbon atoms of a CNT are located at a defect site [Hu et. al., 2001]. A frequently encountered type of defect is so-called Stone–Wales defect, which is comprised of two pairs of 5- and 7-membered rings, and is hence referred to as a 7-5-5-7 defect. A Stone–Wales defect leads to a local deformation of the graphitic sidewall and thereby introduces an increased curvature in this region. The strongest curvature exists at the interface between the 2 5-membered rings; as a result of this curvature, addition reactions are most favored at the carbon–carbon double bonds in these positions [Zhao et. al., 2004].

The EB irradiation procedure results in the formation of carboxylic moieties, preferentially on the end caps of the CNT, since the regions where pentagons are located suffer more strain compared with that of purely hexagonal lattice. Under these conditions, the end caps of the nanotubes are opened and acidic functionalities are formed at these defect sites and at the side walls. The carboxyl groups represent useful sites for further modifications, as they enable the covalent coupling of molecules through the creation of amine or ester bonds (Fig. 8). Isocyanate groups are highly unsaturated organic compounds. They can react readily with many diverse compounds containing active protons such as alcohol, amines and carboxylic acids. Thus, amine-functionalized MWNTs can be obtained where surface-bound isocyanate groups are subsequently reacted with H_2O and converted into amine. The detail of these reactions was summarized as follows. The bisphenol A type low molecular weight epoxy resin (DGEBA, epoxide equivalent weight 121 g/equiv) and PDMS (Mw ≈ 5000) were donated by Huenvi Co., Ltd., Korea and used without further purification. Other chemical compounds were reagent grade and were used as received.

The EB-MWNT and toluene were fed to a glass reactor and the mixture was dispersed for 30 min in an ultrasonic bath at 60°C. Methylene diphenyl diisocyanate (MDI) [diisocyanate terminated polydimethylsiloxane (PDMS) or 3-(triethoxysily)propyl isocyanate (TEPI)], and 1,4-diazabicyclo [2.2.2] octane (DABCO) were added into reactor and the mixture was sonicated for 2 h. Upon completion of the reaction, the mixture was filtered through a filter paper. The filtrate was then washed with toluene and the functionalized MWNT was dried in an oven at 60°C. EB-MWNTs are also reacted with an epoxide to produce an epoxide terminated MWNT. A reaction mixture consisting of toluene, MWNT1200, and DGEBA were charged into the reactor. The mixture was dispersed for 1 h in an ultrasonic bath at 60°C followed by addition of a trace amount of triethylamine as the catalyst. The reaction was carried out for 2 h; then, the mixture was filtered, and the filtrate was washed with toluene and methanol. The filtrate was dried in an oven at 60°C. On the other hand, the covalently functionalized MWNT with PTMG was prepared by using Fischer esterification method [Abuilaiwi et. al, 2010].

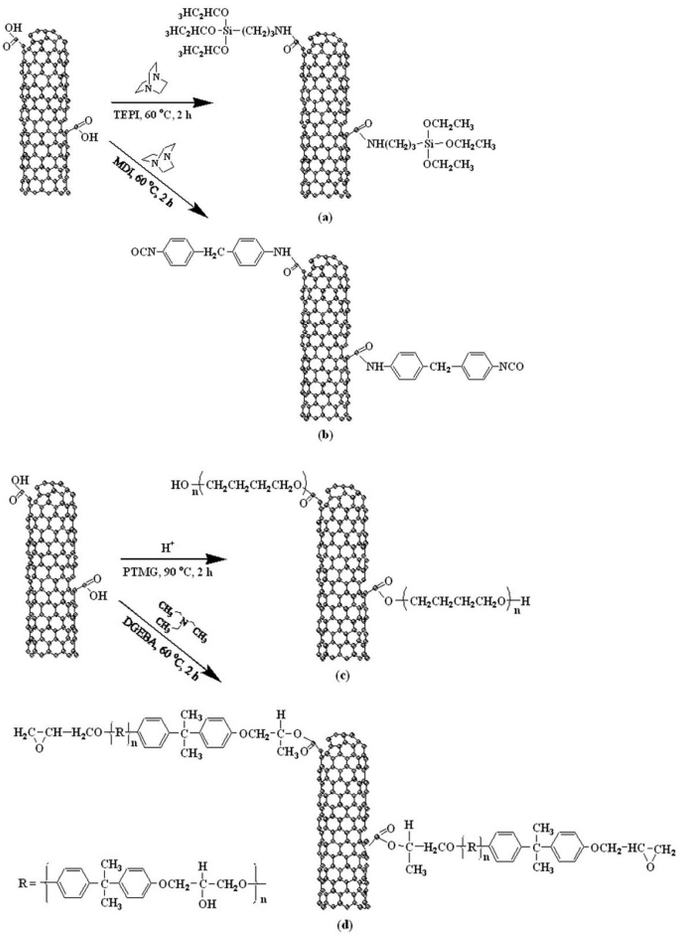

Figure 8. Covalent functionalization EB-MWNT through reaction with TEPI (a), MDI (b), PTMG (c) and DGEBA (d).

Fig. 9 demonstrates the FTIR spectra of the MWNT1200 and covalently functionalized MWNT1200. In the MWNT-TEPI (Fig. 9b), the new bands at 2878 cm^{-1} associated with the stretching of the methylene groups from the TEPI molecules appeared. In addition, the functionalized MWNT shows the peaks of -Si-O-CH_2CH_3 groups at 1175, 1100, 1075, and 970–940 cm^{-1}. As depicted in Fig. 9c, the small peak at 2281 cm^{-1} is from the N−C=O asymmetric vibration, while a new peak is observed at 1544 cm^{-1} which is attributed to the overlapping of a signal from the N−H, N−C bands and N−C=O group [Abuilaiwi et. al., 2010]. The peaks at 3000–2800 cm^{-1} in Fig. 9d are due to C−H antisymmetric and symmetric stretching vibrations of methylene groups of PTMG. The peak at 1460 cm^{-1} originates from the C−H bend of the alkyl chain and the peak at 1108 cm^{-1} arises from the C−O stretch of the ester group. The characteristic epoxy group in synthesized MWNT-DGEBA can be identified on the basis of band presence in the FTIR spectrum 3060-3000 cm^{-1} from -CH vibration of the epoxy ring, 1250 cm^{-1}, from -CO vibrations of the epoxy ring and at 960-815 cm^{-1} from the deformed -CH vibrations of the epoxy ring (Fig. 9e). These results confirmed the attachment of functional molecules onto the EB-MWNT surface.

http://dx.doi.org/10.5772/50883

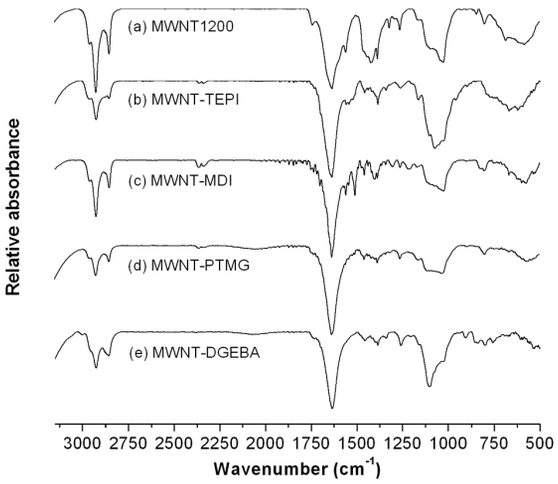

Figure 9. FTIR spectra of the EB-MWNT and covalently functionalized EB-MWNT.

More direct evidence for the covalent functionalization of EB-MWNT is manifested by SEM images. In Fig. 10, SEM images of MWNT1200, MWNT-MDI, MWNT-TEPI, and MWNT-DGEBA are shown. It indicates that the MWNT1200 (Fig. 10a) has a wrinkled and rough surface. However, after covalent functionalization, the wrinkled structures of MWNT1200 were almost disappeared and the surface roughness decreased. These changes in the morphology for MWNT-DGEBA (Fig. 10d) are remarkable. A uniform tubular layer due to covalently bonded DGEBA on the surface of the MWNT1200 is observable. It seems that the average diameters of MWNT-DGEBA are slightly increased in comparison to MWNT1200.

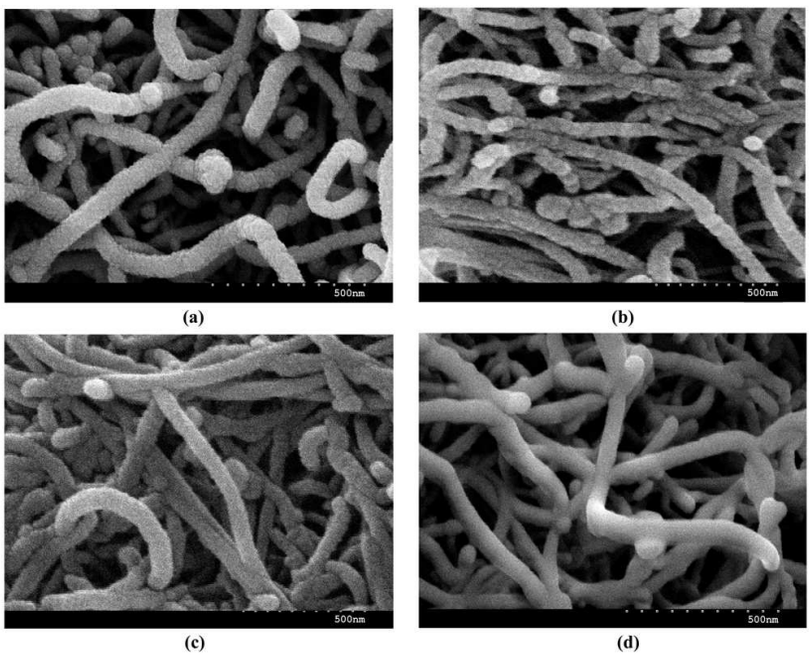

Figure 10. SEM images of the MWNT1200 (a) and covalently functionalized MWNT1200 with MDI (b), TEPI (c), and DGEBA (d).

TGA measurements were conducted on the covalently functionalized EB-MWNT to elucidate their thermal degradation behaviors. Some typical weight-loss curves as a function of temperature are shown in Fig. 11. Several weight loss steps were observed below ~150°C which are due to the release of moisture and the decomposition of the associated organic groups. Fig. 11a, the initial degradation of –COOH group for MWNT1200 starts at approximately 170°C and completes at about 480°C. It also showed no significant weight loss at 480-700°C. Assuming, the portion of the weight loss of functional group at 600°C is the same as that of in the MWNT1200. When the weight loss of the MWNT1200 at 600°C (6.5 %) is used as the reference, the weight loss of covalently functionalized MWNT by TEPI, PDMS, PTMG, and MDI of MWNT-TEPI, MWNT-PDMS, MWNT-PTMG and MWNT-MDI at 600°C is about 4.2, 6.3, 18.8 and 19.8 %, respectively.

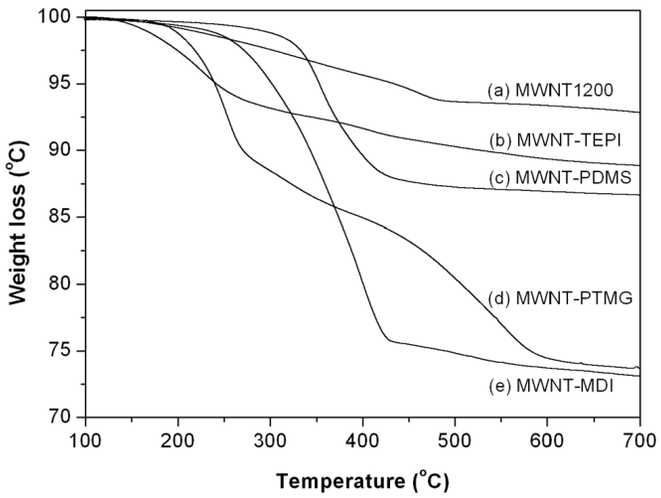

Figure 11. TGA traces of the covalently functionalized EB-MWNT.

3. Applicability of EB-MWNT and covalently functionalized MWNT

The covalent functionalization of CNT has been more interesting because it allows the modification of CNTs surface for subsequent alignment [Tahermansouri et. al., 2010]. The recently developed methods for functionalization of CNTs have opened up a broad range of novel application perspectives. These surface modifications play an important role for application of nanotubes in composite, sensors and many other fields [Chiu and Chang, 2007]. In this section, eight specific applications of EB irradiation and covalently modified MWNTs are described in detail.

3.1. Mechanically reinforced nanocomposites

CNT's polymeric nanocomposites are aimed at the exploitation of the high electrical conductivity of CNTs coupled to high mechanical properties, thermal properties and others unique properties. However, high molecular weight and strong inter-tube forces keep CNT together

http://dx.doi.org/10.5772/50883

in bundles, making their manipulation, characterization and analytical investigation very difficult. Therefore the functionalization of CNTs offers the great advantages of producing soluble and easy-to-handle CNT [Yoon et. al., 2004]. Consequently, compatibility and reactivity of CNT with other material, such as polymer should be strongly improved. Recent work has demonstrated superior dispersion of MWNTs in polymers by functionalization of the nanotubes to compatibilize them with solvents and the matrix polymers [Chiu and Chang, 2007; Wu et. al., 2006; Balasubramanian and Burghard, 2005]. The improved dispersion of nanotubes with functional groups has been accompanied by increased mechanical properties of the nanocomposite. Fig. 12 shows SEM micrographs of the fractured surface of EVA/MWNT and EVA/EB-MWNT nanocomposites after saponification for 6 h and heterogeneous solution reaction in the presence of tetrabutyl titanate (TNBT) catalyst for 20 min. For EVOH/MWNT1200–TNBT [Fig. 12b], the MWNTs dispersed well in the EVOH matrix and most of the MWNTs were broken in the interface rather than pulled out from the polymer matrix. However, the EVOH/MWNT specimen showed a different morphology [Fig. 12a]. Most of the MWNT fibers were pulled out from the EVOH matrix. Such a discrepancy demonstrated that a stronger interfacial adhesion existed between the MWNTs and the EVOH matrix. The presence of the chemical bonding leads to improvement in the mechanical properties of final composite. Consequentially there was about 17% increase in tensile strength for the MWNT1200 nanocomposite compared to pristine MWNT one.

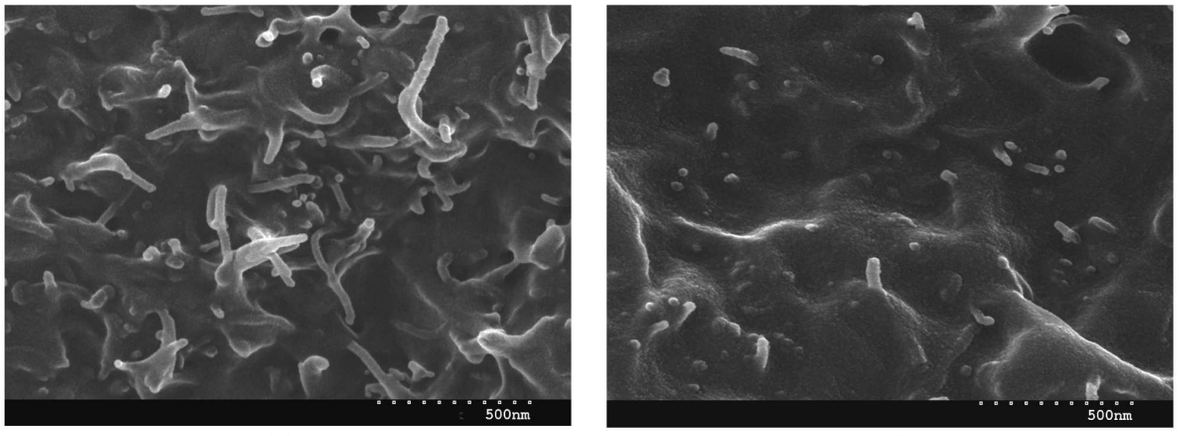

Figure 12. SEM micrographs of the fractured surface of EVA/MWNT and EVA/MWNT1200 nanocomposites (nanotube content = 10 wt%) after saponification for 6 h and heterogeneous solution reaction in the presence of TNBT.

3.2. Inorganic initiator and catalysts

Functionalized nanotubes with different initiator moieties can be used in in-situ polymerizations to produce composites that have covalent bonds between the filler and the polymer chains. They can be produced by incorporating various reactive groups onto the convex surfaces of nanotubes by adjusting the feed ratio of azide compounds to CNTs and were used

in surface-initiated polymerizations, amidation, and reduction of metal ions affording various CNT-polymer and CNT-Pt nanohybrids [Liu and Chen, 2007; Sahoo et. al., 2010]. For example, CNTs functionalized by butyl lithium act as an initiator for polymerization to produce grafted CNT polymer nanocomposites where the anions disperse the nanotubes due to electrostatic repulsive force between the tubes [Abuilaiwi et al., 2010]. When CNTs are functionalized by oxy radicals, they also act as initiators for polymerization of polyethylene chains grafted on the CNTs [Gao et. al., 2009]. MWNT with hydroxyl groups can be used as co-initiators to polymerize poly(ε-caprolactone) or poly(α-chloro-ε-caprolactone) by surface-initiated ring-opening polymerization. Pendent chlorides were converted into azides by the reaction with sodium azides. Finally, various types of terminal alkynes were reacted with pendent azides by copper-catalyzed Huisgen's 1,3-dipolar cycloaddition [Lee, et. al., 2011]. Moreover, for a long time, active carbon has found wide spread application as a support material in heterogeneous catalysis. Compared to this form of carbon, CNTs offer the advantage of a more defined morphology and chemical composition as well as the possibility to attach catalysts onto their surface through covalent bonds [Balasubramanian and Burghard, 2008]. The applicability of CNTs as carriers for catalytically active molecular functional units has recently been demonstrated through the covalent coupling of an organic vanadyl complex [Baleizão et. al., 2004].

3.3. Drug delivery and gene therapy

A drug delivery systems are continuously being developed to improve the pharmacological profile and the therapeutic properties of administered drugs [Allen and Cullis, 2004; Shohet et. al., 2000; Davis, 1997]. They have been developed according to the different classes of bioactive molecules to be delivered and the characteristics of the target tissues. Liposomes, emulsions, cationic polymers, micro and nanoparticles are the most commonly studied vehicles [Singh, et. al., 2010]. MWNTs can be functionalized by attaching biological molecules such as different peptides, proteins, nucleic acids and small organic molecules are able to deliver their cargos into cells, thus opening the path for their facile manipulation and processing in physiological environments. For instance, enzymes which contain many amine and hydroxyl groups react with isocyanate groups in MWNT-NCO thereby forming covalently bound enzymes. Then they can usefully mimic certain biological functions, such as drug delivery and gene therapy. Because large part of the human body consists of carbon, CNTs are generally thought of as a very biocompatible material [Singh, et. al., 2010]. Cells have been shown to grow on CNTs so they appear to have no toxic effect. The cells also do not adhere to the CNTs, potentially giving rise to application such as coatings for prosthetics. The molecular targeting of CNT delivery systems derivatised with a therapeutic agent is possible if an active recognition moiety is simultaneously present at the surface of the carrier [Kam et. al., 2005]. Moreover attachment of a fluorescent molecule would provide optical signals for imaging and localisation of the CNT–drug conjugates [Pastorin et. al., 2006]. The ability to functionalize the sidewalls of CNTs also leads to biomedical application such as vascular stents, neuron growth and regeneration [Guzman et. al., 1996].

http://dx.doi.org/10.5772/50883

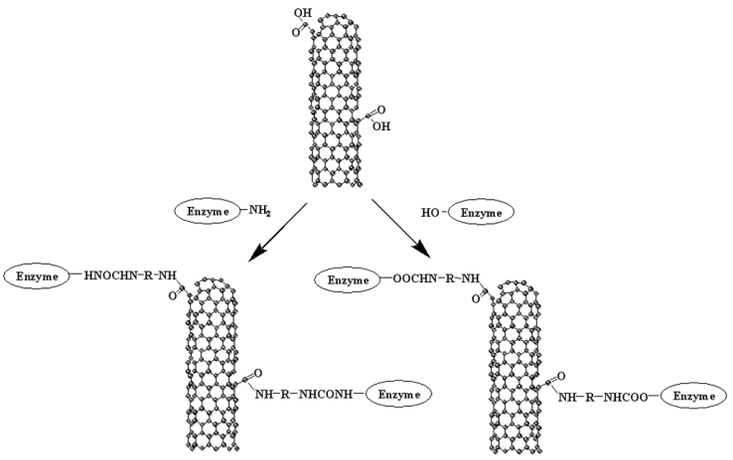

Figure 13. Immobilization of enzymes onto isocyanate functionalized MWNT.

3.4. Energy storage and conversion device

Self-assembly is a process that occurs due to the spontaneous and uninstructed structural reorganization that forms from a disordered system. Such processes are reversible and held together by non-covalent intermolecular forces. Layer-by-layer (LBL) assembly is a versatile method to form dense thin films from dispersed solutions containing functionalized nanomaterials. This technology takes advantage of the charge-charge interaction between substrate and monolayers to create multiple layers held together by electrostatic forces. The LBL approach consists of the repeated, sequential immersion of a substrate into aqueous solutions of functionalized materials having complementary charge, thereby producing conformal ultra-thin films and controllable surface morphology using various nanomaterials. Electrostatic LBL assembly, in which CNTs have been alternated with polymers for various energy storage and conversion devices, has exhibited improved networks for electrochemical energy applications. Recently, Lee and co-workers [Lee, et. al., 2009] reported the preparation of MWNT thin films based on the LBL assembly method. The authors prepared negatively and positively charged MWNTs by surface functionalization using carboxylic acid and amine groups, respectively. The complementary charged and functionalized MWNT dispersions enable the incorporation of MWNTs into highly controlled thin films using LBL assembly. The prepared MWNT exhibited high electronic conductivity in comparison with polymer composites with SWNTs, and high capacitive behaviour with the ability to precisely control the capacity [Lee, et. al., 2009]. The average capacitance was considerably higher than those of vertically aligned or conventional CNT electrodes due to the high nanotube densities and well developed nanopores in the LBL MWNT thin films. This study indicates the potential to precisely control the charge and energy storage parameters in MWNT thin films by controlling the number of bilayers and film thickness in the LBL assembly. Therefore precise control of the LBL system can be used to design ideal electrode materials for fuel cells, photoelectrochemical cells, batteries, supercapacitors [Lee, et. al., 2009], and strain and corrosion sensing [Loh, et. al, 2007].

3.5. Nanofiltration membrane for purification and separation

Nanofiltration is a relatively recent membrane filtration process used most often with low total dissolved solids water such as surface water and fresh groundwater, with the purpose of softening and removal of disinfection by-product precursors [Raymond, 1999]. The development of advanced membrane technologies with controlled and novel pore architectures is important for the achievement of more efficient and cost effective purification. Present polymeric membranes are well known to suffer from a trade off between selectivity and permeability, and in some cases are also susceptible to fouling or exhibit low chemical resistance [Sears, et. al., 2010]. Modification of membrane surfaces through the introduction of nano materials is another strategy to reduce fouling, or to alter the affinity of the membrane for organic solutes. One premise of the current effort if that these properties might be exploited to create membrane materials of very high strength. MWNTs exhibit characteristics such as strength, and thermal and electrical conductivity that make them promising materials for use in developing new nanocomposite materials. Moreover their toxicity might be exploited when inserted in membranes as a basis for inhibiting bacterial growth and therefore reducing biofouling. Such toxic effects towards bacteria were detected MWNT immobilized within the membrane skin might serve as a basis for fouling produced by microbial growth.

Recently, our group has developed a process of simple saponification to make highly porous nanocomposites [Lee et. al, 2012]. In this process, at least one vinyl acetate (VAc) containing polymer or blend is dissolved in an appropriate solvent and a suitable viscosity of the solution is achieved. EB-irradiated MWNT was dispersed in polymer solution and then the polymer suspension was precipitated and saponified in alkaline non-solvent. After rinsing off the coagulant and drying, sponge-like structure of connected matrix polymer and nanotube were obtained. Production parameters that affect the pore structure and properties include polymer and nanotube concentration, VAc content in polymer, saonification time and temperature, and precipitation media. These factors can be varied to produce porous structure with a large range of pore sizes, and altering chemical, thermal and mechanical properties. These nanocomposites with highly porous and excellent antibacterial activity have potential use of nanofiltration membranes in treatment of industrial wastewater and removal of disinfection (Fig. 14).

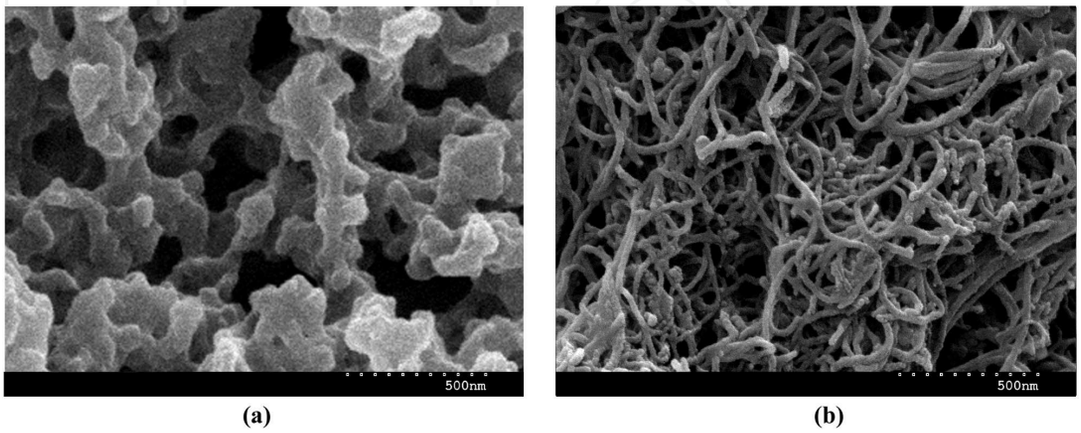

Figure 14. SEM micrographs of the PVA (a) and PVA/MWNT1200 (b) nanocomposite particle prepared by simple saponification method using ethanol/NaOH solution.

http://dx.doi.org/10.5772/50883

3.6. Antibacterial agents

The microbial contaminated materials could serve as important sources of cross-infections, causing a variety of serious consequences in medical devices, hospital equipment, water purification and delivery systems, bio-protective equipment. Even though they cannot be directly assimilated by microorganisms, microbes can grow and propagate using bioassimilable contaminants on the surface of the polymeric materials. One possible way to avoid microbial contamination is to develop materials that possess antimicrobial activities [Park et. al., 2001; Park et. al., 2001; Moon et. al., 2003, Moon et. al., 2003; Park et. al., 2004; Park et. al., 2004; Kim et. al., 2004; Yang and Park, 2006; Park et. al., 2008]. Moreover, increased efficiency, selectivity, and handling safety are additional benefits which may be realized [Kim et. al., 2004]. Antimicrobial agents used in antimicrobial-processed products are classified into organic, inorganic and natural organic compounds. Organic antimicrobial agents raise health concerns and many of them do not have sufficient antimicrobial activity. Polymeric biocides can significantly reduce loss of antimicrobial activity associated with volatilization, photolytic decomposition, dissolution, and permeation [Kim et. al., 2004]. On the other hand, inorganic antimicrobial agents employ Ag, Cu, and Zn compounds and are excellent in safety and antimicrobial activity. These metalic compounds are used in many types of household and medical products due to their good balance between antimicrobial activity and endurance. However, patients with metal allergy due to Cu or Zn have been reported [Nakashima et. al., 2008].

As previously mentioned, CNTs possess antimicrobial properties themselves, and their relevant activities were ascribed to the behavior of 'nanodart' with the proposed physical damage mechanism [Kang et. al., 2008]. The intrinsic toxicity of CNT depends on the degree of surface functionalization and the different toxicity of functional groups. In the presence of water, the isocyanate groups in MWNT can react with water. The reaction is a three step process (Fig. 15). A water molecule reacts with an isocyanate group to form cabamic acid. Carbamic acids are unstable, and decompose forming CO_2 and an amine. Existence of high abundance of amine groups on the surface of functionalized MWNTs provided sites for binding of various antibiotics such like norfloxacin, and for formation of silver nanoparticles by the reduction of aqueous solution of $AgNO_3$.

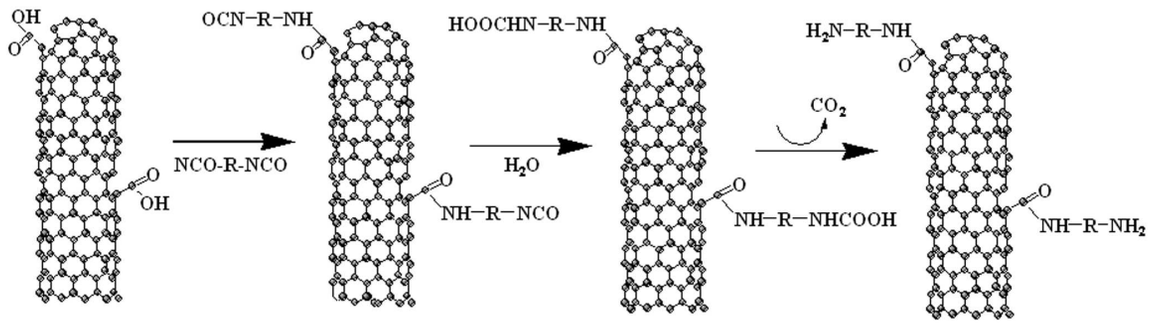

Figure 15. Synthesis of amine covalently functionalized MWNT.

Recently, Neelgund and Oki synthesized the nanohybrids composed of silver nanoparticles and aromatic polyamide functionalized MWNTs. Prior to deposition of silver nanoparticles, acid treated MWNTs were successively reacted with p-phenylenediamine and methylmethacrylate to form series of NH_2-terminated aromatic polyamide dendrimers on the surface of MWNTs through Michael addition and amidation. The antimicrobial activity of MWNT-Ar-NH_2/Ag nanohybrids were measured against *E. coli*, *P. aeruginosa* and *S. aureu* and compared with MWNT-COOH and MWNT-Ar-NH_2. The results showed that functionalization of MWNTs with aromatic polyamide dendrimers and successive deposition of Ag nanoparticles could play an important role in the enhancement of antimicrobial activity [Neelgund and Oki, 2011].

3.7. Environmental friendly aqueous coating system

For coating applications a uniform and stable dispersion of particulate matter plays an important role. This requirement is especially critical when submicron or nano-sized particles are involved. CNTs tend to cohere in aqueous dispersion due to their high surface energy and lack of chemical affinity with the dispersing medium [Park et. al., 2002]. Surfactant adsorption on nanotube surfaces and chemical functionalization of nanotube sidewalls are two of the most widely-used methods for solubilization of nanotubes. Non-covalent surface treatment by surfactants or polymers has been used in the preparation of both aqueous and organic solutions to obtain high weight fraction of individually dispersed nanotubes [Barraza et. al., 2002; Jiang et. al., 2003; Yurekli et. al., 2004]. When surfactants are employed in CNT dispersions, surfactant molecules work by adsorption at the interface and self-accumulation into supra-molecular structures, which help their dispersion retain a stable colloidal state. However, surfactants adsorbed on nanotubes create a physical barrier between the nanotubes and the environment [Hobbie et. al., 2006; Lee et. al., 2007]. Chemical methods use surface functionalization of CNT to improve their chemical compatibility with the target medium that is to enhance wetting and reduce their tendency to agglomerate [Vaisman et. al., 2006]. Systematic investigation of the effects of nanotube length and functionalization for MWNT has revealed that the introduction of carboxylic or thiol groups on the surface of shortened nanotubes increases the stability of MWNT dispersions up to 0.24 mg/ml. Octadecyl-amide functionalized MWNT were reported to exhibit good solubility in polar solvents [Qin et. al., 2003]. These long chain alkylamide-functionalized nanotubes were obtained where surface-bound COOH groups are converted into thionyl chloride groups and subsequently reacted with amine. The introduction of surface charge on MWNT also has contrasting effects on stabilising their dispersions. MWNTs are modified with carboxylic anion groups; the dispersion stability in water was significantly enhanced due to the combination of polar–polar affinity and electrostatic repulsion [Lee et. al., 2007]. MWNT uniformly dispersed in water can be utilized in environmental friendly aqueous coating, direct conductive coating, further sol–sol process and aqueous nanocomposite system.

http://dx.doi.org/10.5772/50883

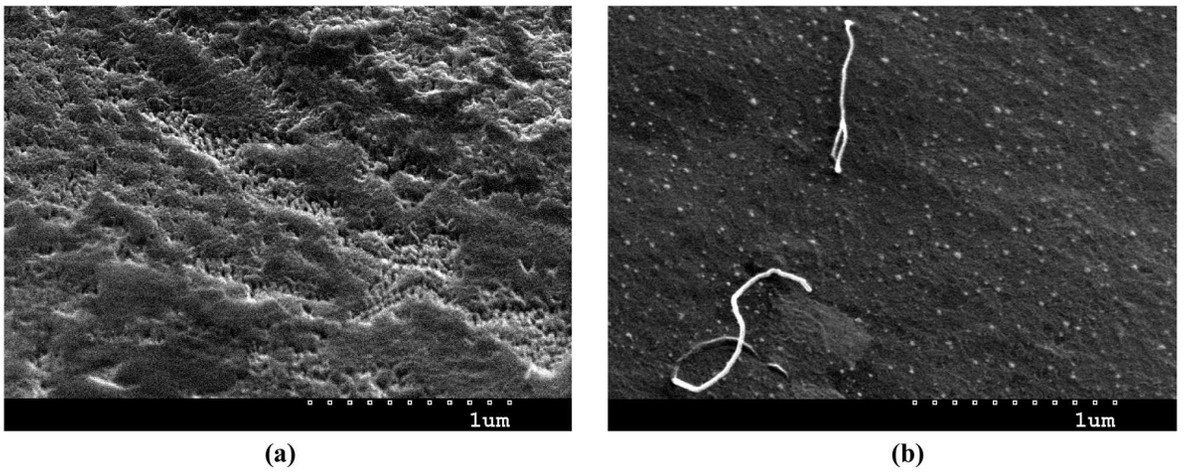

Figure 16. SEM image of the sodium silicate (a) and sodium silicate/functionalized MWNT composites prepared from aqueous coating system (b).

3.8. Electromagnetic interference (EMI) shielding materials

As electromagnetic radiation, particularly that at high frequencies tend to interfere with electronics, EMI shielding of both electronics and radiation source is needed and is increasingly required by governments around the world [Chung, 2001]. The radiation may be either electromagnetic in nature, such as X-rays and gamma rays, or charged particles, such as beta particles and electrons. The lifetime and efficiency of them can be increased by the effective shielding. Generally, highly electroconductive materials such like metals are used for shielding application. However, metals have their own shortcomings like heavy weight, susceptibility to corrosion, wear, and physical rigidity [Wu et al., 2006]. Many researches have been conducted to improve the EMI shielding of polymer materials by coating an electroconductive layer on the surface, incorporating electroconductive fillers, or utilizing electroconductive polymers. Among various electroconductive fillers that have been utilized, covalently functionalized MWNT is one of the most promising candidates, not only because of its good electrical conductivity but also because of its ability to improve mechanical properties. Recently, the mass production of MWNTs causes price reduction. They are more affordable for application in nanocomposites [Wu et. al., 2006].

4. Conclusion

Current interest in CNTs has been generated and maintained because nanotubes exhibit unique properties include high modulus, high aspect ratios, excellent thermal and electrical conductivities, and magnetic properties not achievable with traditional filler. In this chapter, MWNTs were subjected to EB irradiation at various doses to determine the incidence of surface modification and, resultantly, deformation or destruction to the otherwise pristine graphitic structure. FTIR spectra obtained from EB-MWNT samples provide insight into the

level of surface modification. The introduced carboxyl groups represent useful sites for further modifications, as they enable the covalent coupling of molecules through the creation of ester or amide bonds. Consequently, EB-MWNT was covalently functionalized with isocyanate, epoxy, and hydroxyl compounds and their applicability was investigated. As has been shown in this study, the possible applications of them range widely, from nanocomposite materials to antibacterial agents. Functional groups such like isocyanate group on MWNT surface can interact with -OH group in polymers by urethane bonding and result in a better dispersion of MWNT in polyurethane matrix. Afterward we carry out extensive studies to investigate the properties and applicability for urethane link polydimethylsiloxane/MWNT nanocomposites using various isocyanate functionalized MWNT.

Acknowledgements

We are grateful to the Small and Medium Enterprises (SMEs) Technology Innovation Program, Republic of Korea, for financial support of this experimental work.

Author details

Eun-Soo Park[1*]

Address all correspondence to: t2phage@hitel.net

1 Youngchang Silicone Co., Ltd., Korea

References

[1] Abuilaiwi, F. A., Laoui, T., Al-Harthi, M., & Atieh, M. A. (2010). Modification and functionalization of multiwalled carbon nanotube (MWCNT) via Fischer esterification. *The Arabian Journal for Science and Engineering*, 35, 38-48.

[2] Ajayan, P., Stephan, O., Colliex, C., & Trauth, D. (1994). Aligned carbon nanotube arrays formed by cutting a polymer resin-nanotube composite. *Science*, 265(5176), 1212-1214.

[3] Allen, T. M., & Cullis, P. R. (2004). Drug delivery systems: entering the mainstream. *Science*, 303, 1818-1822.

[4] Balasubramanian, K., & Burghard, M. (2008). Electrochemically functionalized carbon nanotubes for device applications. *Journal of Materials Chemistry*, 18, 3071-3083.

[5] Baleizão, C., Gigante, B., Garcia, H., & Corma, A. (2004). Vanadyl salen complexes covalently anchored to single wall carbon nanotubes as heterogeneous catalyst for the cyanosilylation of aldehydes. *Journal of Catalysis*, 221, 77-84.

[6] Banerjee, S., Hemraj-Benny, T., & Wong, S. S. (2005). Covalent surface chemistry of single-walled carbon nanotubes. *Advanced Materials*, 17, 17-29.

[7] Banhart, F. (1999). Irradiation Effects in Carbon Nanostructures. *Reports on Progress in Physics*, 62, 1181-1221.

[8] Barraza, H. J., Pompeo, F., O'Rear, E. A., & Resasco, D. E. (2002). SWNT-filled thermoplastic and elastomeric composites prepared by miniemulsion polymerization. *Nano Letters*, 2, 797-802.

[9] Basiuk, E. V., Monroy-Pelaez, M., Puente-Lee, I., & Basiuk, V. A. (2004). Direct solvent-free amination of closed-cap carbon nanotubes: A link to fullerene chemistry. *Nano Letters*, 4, 863-866.

[10] Burghard, M., & Balasubramanian, K. (2005). Chemically Functionalized Carbon Nanotubes. *Small*, 1(2), 180-192, DOI:10.1002/smll.200400118.

[11] Chen, L., Xie, H., & Yu, W. (2011). *Functionalization Methods of Carbon Nanotubes and Its Applications In Carbon Nanotubes Applications on Electron Devices*, Mauricio, J. M., Eds, 213-232, 978-9-53307-496-2.

[12] Chiu, W. M., & Chang, Y. A. (2007). Chemical modification of multiwalled carbon nanotube with the liquid phase method. *Journal of Applied Polymer Science*, 107, 1655-1660, DOI:10.1002/app.26633.

[13] Chung, D. D. L. (2001). Electromagnetic interference shielding effectiveness of carbon. *Carbon*, 39, 279-285.

[14] Davis, S. S. (1997). Biomedical applications of nanotechnology-implications for drug targeting and gene therapy. *Ophthalmic Genetics*, 15, 217-224.

[15] Donaldson, K., Stone, V., Tran, C. L., Kreyling, W., & Borm, P. J. A. (2009). Nanotoxicology. *Occupational and Environmental Medicine*, 61, 727-728.

[16] Dresselhaus, G., & Avouris, P. (2001). Eds, *Carbon Nanotubes: Synthesis, Structure, Properties and Applications*, 80, Springer-Verlag, Berlin, 81-112.

[17] Gao, C., He, H., Zhou, L., Zheng, X., & Zhang, Y. (2009). Scalable Functional Group Engineering of Carbon Nanotubes by Improved One-Step Nitrene Chemistry. *Chemistry of Materials*, 21, 360-370.

[18] George, J. J., & Bhowmick, A. K. (2009). Influence of Matrix Polarity on the Properties of Ethylene Vinyl acetate-carbon nanofiller nanocomposites. *Nanoscale Research Letters*, 4, 655-664, DOI:10.1007/s11671-009-9296-8.

[19] Guzman, L. A., Labhasetwar, V., Song, C., Jang, Y., Lincoff, A. M., Levy, R., & Topol, E. J. (1996). Local intraluminal infusion of biodegradable polymeric nanoparticles. A novel approach for prolonged drug delivery after balloon angioplasty. *Circulation*, 94, 1441-1448.

[20] Harris, P. J. F. (2004). Carbon nanotube composites. *International Materials*, 49(1), 31-43, DOI: 10.1179/095066004225010505.

[21] Hirsch, A. (2002). Functionalization of Single-Walled Carbon Nanotubes. *Angewandte Chemie International Edition*, 41, 1853-1859.

[22] Hobbie, E. K., Obrzut, J., Kharchenko, S. B., & Grulke, E. A. (2006). Charge transport in melt-dispersed carbon nanotubes. *Journal of Chemical Physics*, 125, 044712-1-044712-3.

[23] Hogt, A. H., Dankert, J., & Feijen, J. (1986). Adhesion of coagulase-negative staphylococci to methacrylate polymers and copolymers. *Journal of Biomedical Materials Research*, 20, 533-545.

[24] Hu, H., Bhowmik, P., Zhao, B., Hamon, M. A., Itkis, M. E., & Haddon, R. C. (2001). Determination of the acidic sites of purified single-walled carbon nanotubes by acid-base titration. *Chemical Physics Letters*, 345, 25-28.

[25] Jia, G., Wang, H. F., Yan, L., Wang, X., Pei, R. J., Yan, T., Zhao, Y. L., & Guo, X. B. (2005). Cytotoxicity of Carbon Nanomaterials: Single-Wall. Nanotube, Multi-Wall Nanotube, and Fullerene. *Environmental Science & Technology*, 39, 1378-1383.

[26] Jiang, L., Gao, L., & Sun, J. (2003). Production of aqueous colloidal dispersions of carbon nanotubes. *Journal of Colloid and Interface Science*, 260, 89-94.

[27] Jucker, B. A., Harms, H., & Zehnder, A. B. (1996). Adhesion of the positively charged bacterium Stenotrophomonas (Xanthomonas) maltophilia 70401 to glass and Teflon. *Journal of Bacteriology*, 178, 5472-5479.

[28] Kam, N. W. S., Connel, M. O'., Wisdom, J. A., & Dai, H. (2005). Carbon nanotubes as multifunctional biological transporters and near-infrared agents for selective cancer cell destruction. *PNAS*, 102, 11600-11605.

[29] Kang, S., Herzberg, M., Rodrigues, D. F., & Elimelech, M. (2008). Antibacterial Effects of Carbon Nanotubes: Size Does Matter! *Langmuir*, 24, 6409-6413, DOI: 10.1021/la800951v.

[30] Kanny, K., Muhfuz, H., Carlsson, L. A., Thomas, T., & Jeelani, S. (2002). Dynamic mechanicalanalyses and flexural fatigue of PVC foams. *Composite Structures*, 58, 175-183.

[31] Kim, J. H., Park, E. S., Shim, J. H., Kim, M. N., Moon, W. S., Chung, K. H., & Yoon, J. S. (2004). Antimicrobial activity of p-hydroxyphenyl acrylate derivatives. *Journal of Agricultural and Food Chemistry*, 52, 7480-7483.

[32] Kim, G. T., & Park, E. S. (2008). Thermal Reproducibility and Voltage Stability of Carbon Black/Multiwalled Carbon Nanotube and Carbon Black/SnO_2-Sb Coated Titanium Dioxide Filled Silicone Rubber Heaters. *Journal of Applied Polymer Science*, 109, 1381-1387, DOI:10.1002/app.28200.

[33] Krasheninnikov, A. V., & Nordlund, K. (2004). Irradiation effects in carbon nanotubes. *Nuclear Instruments and Methods in Physics Research*, B216, 355-366.

[34] Krijgsman, J. (1992). *Product Recovery in Bioprocess Technology*, Butterworth-Heinemann, 0-75061-510-9.

[35] Kumar, S., Doshi, H., Srinivasarao, M., Park, J. O., & Schiraldi, D. A. (2002). Fibers from polypropylene/nano carbon fiber composites. *Polymer*, 43, 1701-1703.

[36] Lau, A. K.-T., & Hui, D. (2002). The Revolutionary Creation of New Advanced Materials: Carbon Nanotube Composites. *Composites Part B: Engineering*, 33(2), 263-267.

[37] Li, Q. W., Li, Y., Zhang, X. F., Chikkannanavar, S. B., Zhao, Y. H., Dangelewicz, A. M., Zheng, L. X., Doorn, S. K., Jia, Q. X., Peterson, D. E., Arendt, P. N., & Zhu, Y. T. (2007). Structure-Dependent Electrical Properties of Carbon Nanotube Fibers. *Advanced Materials*, 19, 3358-3363, DOI: 10.1002/adma.200602966.

[38] Liu, Y.-L., & Chen, W.-H. (2007). Modification of Multiwall Carbon Nanotubes With Initiators and Macroinitiators of Atom Transfer Radical Polymerization. *Macromolecules*, 40, 8881-8886.

[39] Lee, E. J., Yoon, J. S., & Park, E. S. (2011). Morphology, Resistivity, and Thermal Behavior of EVOH/Carbon Black and EVOH/Graphite Composites Prepared by Simple Saponification Method. *Polymer Composites*, 32, 714-726.

[40] Lee, E. J., Yoon, J. S., & Park, E. S. (2012). Preparation and Properties of the Highly Porous Poly(ethylene-co-vinyl alcohol)/Multiwalled Carbon Nanotube Nanocomposites Prepared by a Simple Saponification Method. *Journal of Applied Polymer Science*, 125, E691-E704, DOI: 10.1002/app.36537.

[41] Lee, J. W., Kim, M. H., Hong, C. K., & Shim, S. E. (2007). Measurement of the dispersion stability of pristine and surface-modified multiwalled carbon nanotubes in various nonpolar and polar solvents. *Measurement Science and Technology*, 18, 3707-3712, doi:10.1088/0957-0233/18/12/005.

[42] Lee, K., Li, L., & Dai, L. (2005). Asymmetric end-functionalization of multiwalled carbon nanotubes. *Journal of the American Chemical Society*, 127, 4122-4123.

[43] Lee, R. S., Chen, W. H., & Lin, J. H. (2011). Polymer-grafted multi-walled carbon nanotubes through surface-initiated ring-opening polymerization and click reaction. *Polymer*, 52, 2180-2188.

[44] Lee, S. W., Kim, B. S., Chen, S., Shao-Horn, Y., & Hammond, P. T. (2009). Layer-by-Layer Assembly of All Carbon Nanotube Ultrathin Films for Electrochemical Applications. *Journal of the American Chemical Society*, 131, 671-679, DOI: 10.1021/ja807059k.

[45] Lewinski, N., Colvin, V., & Drezek, R. (2008). Cytotoxicity of Nanoparticles. *Small*, 4(1), 26-49.

[46] Loh, K. J., Kim, J., Lynch, J. P., Kam, N. S., & Kotov, N. A. (2007). Multifunctional layer-by-layer carbon nanotube-polyelectrolyte thin films for strain and corrosion sensing. *Smart Materials and Structures*, 16, 429-438.

[47] Moon, W. S., Chung, K. H., Seol, D. J., Park, E. S., Shim, J. H., Kim, M. N., & Yoon, J. S. (2003). Antimicrobial effect of monomers and polymers with azole moieties. *Journal of Applied Polymer Science*, 90, 2933-2937.

[48] Moon, W. S., Kim, J. C., Chung, K. H., Park, E. S., Kim, M. N., & Yoon, J. S. (2003). Antimicrobial activity of a monomer and its polymer based on quinolone. *Journal of Applied Polymer Science*, 90, 1797-1801.

[49] Meyyappan, M., Yamada, T., Sarrazin, P., & Li, J. (2005). *Carbon Nanotubes: Science and Applications*, CRC Press.

[50] Nakashima, H., Miyano, N., & Takatuka, T. (2008). Elution of metals with artificial sweat/saliva from inorganic antimicrobials/processed cloths and evaluation of antimicrobial activity of cloths. *Journal of Health Science*, 54, 390-399.

[51] Neelgund, G. M., & Oki, A. (2011). Deposition of Silver Nanoparticles on Dendrimer Functionalized Multiwalled Carbon Nanotubes: Synthesis, Characterization and Antimicrobial Activity. *Journal of Nanoscience and Nanotechnology*, 11(4), 3621-3629.

[52] Nel, A., Xia, T., Madler, L., & Li, N. (2006). Toxic Potential of Materials at the Nanolevel. *Science*, 311, 622-627.

[53] Okaya, T., & Ikari, K. (1997). *Polyvinylalcohol-Development*, Finch, C. A. (Ed.), John Wiley & Sons, 978-0-47199-850-1, Chichester (Chapter 8).

[54] Park, C., Oundaies, Z., Watson, K. A., Crooks, R. E., Smith, J. Jr., Lowther, S. E., Connell, J. W., Siochi, E. J., Harrison, J. S., & St Clair, T. L. (2002). Dispersion of single wall carbon nanotubes by in-situ polymerization under sonication. *Chemical Physics Letters*, 364, 303-308.

[55] Park, E. S. (2008). Mechanical properties and antibacterial activity of peroxide-cured silicone rubber foams. *Journal of Applied Polymer Science*, 110, 1723-1729.

[56] Park, E. S., Kim, H. K., Shim, J. H., Kim, M. N., & Yoon, J. S. (2004). Synthesis and properties of polymeric biocides based on poly ethylene-co-vinyl alcohol. *Journal of Applied Polymer Science*, 93, 765-770.

[57] Park, E. S., Kim, H. S., Kim, M. N., & Yoon, J. S. (2004). Antibacterial activities of polystyrene-block-poly(4-vinyl pyridine) and poly(styrene-random-4-vinyl pyridine). *European Polymer Journal*, 40, 2819-2822.

[58] Park, E. S., Lee, H. J., Park, H. Y., Kim, M. N., Chung, K. H., & Yoon, J. S. (2001). Antifungal effect of carbendazim supported on poly(ethylene-co-vinyl alcohol) and epoxy resin. *Journal of Applied Polymer Science*, 80, 728-736.

[59] Park, E. S., Moon, W. S., Song, M. J., Kim, M. N., Chung, K. H., & Yoon, J. S. (2001). Antimicrobial activity of phenol and benzoic acid derivatives. *International Biodeterioration & Biodegradation*, 47, 209-214.

[60] Pastorin, G., Wu, W., Wieckowski, S., Briand, J. P., Kostarelos, K., Prato, M., & Bianco, A. (2006). Double functionalisation of carbon nanotubes for multimodal drug delivery. *Chemical Communications*, 1182-1184.

[61] Petrova, S., Miloshev, S., Mateva, R., & Iliev, I. (2008). Synthesis of Amphiphilic PEG-PCL-PEG Triblock Copolymers. *Journal of the University of Chemical Technology and Metallurgy*, 43, 199-204.

[62] Qin, Y., Liu, L., Shi, J., Wu, W., Zhang, J., Guo, Z. X., Li, Y., & Zhu, D. (2003). Large Scale Preparation of Solubilized Carbon Nanotubes. *Chemistry of Materials*, 15, 3256-3260.

[63] Ramanathan, T., Stankovich, S., Dikin, D. A., Liu, H., Shen, H., & Nguyen, S. T. (2007). Graphitic nanofillers in PMMA nanocomposites-An investigation of particle size and dispersion and their influence on nanocomposite properties. *Journal of Polymer Science Part B: Polymer Physics*, 45, 2097-2112.

[64] Radovic, L. R. (2003). *Chemistry and Physics of Carbon*, Marcel Dekker, New York, USA.

[65] Raymond, D. L. (1999). *Water Quality and Treatment*, 5th, American Water Works Association and McGraw-Hill, New York, 0-07001-659-3.

[66] Sahoo, N. G., Rana, S., Cho, J. W., Li, L., & Chan, S. H. (2010). Polymer Nanocomposites Based on Functionalized Carbon Nanotubes. *Prog. Polym. Sci.*, 35, 837-867.

[67] Salvetat, J. P., Bonard, J. M., Thomson, N. H., Kulik, A. J., Forro, L., Benoit, W., & Zuppiroli, L. (1999). Mechanical properties of carbon nanotubes. *Applied Physics A*, 69, 255-260.

[68] Sears, K., Dumée, L., Schütz, J., She, M., Huynh, C., Hawkins, S., Mikel, M., & Gray, S. (2010). Recent Developments in Carbon Nanotube Membranes for Water Purification and Gas Separation. *Materials*, 3, 127-149, DOI:10.3390/ma3010127.

[69] Shohet, R. V., Chen, S., Zhou, Y. T., Wang, Z., Meidell, R. S., Unger, R. H., & Grayburn, P. A. (2000). Echocardiographic destruction of albumin microbubbles directs gene delivery to the myocardium. *Circulation*, 101, 2554-2556.

[70] Singh, P., Tripathi, R. M., & Saxena, A. (2010). Synthesis of carbon nanotubes and their biomedical applications. *Journal of Optoelectronics and Biomedical Materials*, 2, 91-98.

[71] Szleifer, I., & Yerushalmi-Rozen, R. (2005). Polymers and carbon nanotubes- dimensionality, interactions and nanotechnology. *Polymer*, 46(19), 7803-7818, 0032-3861.

[72] Tahermansouri, H., Chobfrosh khoei, D., & Meskinfam, M. (2010). Functionalization of Carboxylated Multi-wall Nanotubes with 1,2-phenylenediamine. *International Journal of Nano Dimension*, 1, 153-158, 2008-8868.

[73] Thostenson, Erik T., Zhifeng, Ren., & Tsu-Wei, Chou. (2001). Advances in the science and technology of carbon nanotubes and their composites: a review. *Composite Science and Technology*, 61, 1899-1912.

[74] Thostenson, E. T., & Chou, T. W. (2002). Aligned multi-walled carbon nanotube-reinforced composites: processing and mechanical characterization. *Journal of Physics D: Applied Physics*, 35(16), L77-L80.

[75] Treacy, M. M. J., Ebbesen, T. W., & Gibson, J. M. (1996). Exceptionally high Young's modulus observed for individual carbon nanotubes. *Nature*, 381(6584), 678-680.

[76] Vaisman, L., Wagner, H. D., & Marom, G. (2006). The role of surfactants in dispersion of carbon nanotubes. *Advances in Colloid and Interface Science*, 128-130, 37-46.

[77] Vaisman, L., Wachtel, E., Wagner, H. D., & Marom, G. (2007). Polymer-nanoinclusion interactions in carbon nanotube based polyacrylonitrile extruded and electrospun fibers. *Polymer*, 48, 6843-6854.

[78] Wong, S. S., Joselevich, E., Wooley, A. T., Cheung, C. L., & Lieber, C. M. (1998). Covalently functionalized nanotubes as nanometre-sized probes in chemistry and biology. *Nature*, 394, 52-55.

[79] Wong, E. W., Sheehan, P. E., & Lieber, C. M. (1997). Nanobeam Mechanics: Elasticity, Strength, and Toughness of Nanorods and Nanotubes. *Science*, 277(5334), 1971-1975.

[80] Wu, H. L., Ma, C. C. M., Yang, Y. T., Kuan, H. C., Yang, C.-C., & Chiang, C. L. (2006). Morphology, Electrical Resistance, Electromagnetic Interference Shielding and Mechanical Properties of Functionalized MWNT and Poly(urea urethane) Nanocomposites. *Journal of Polymer Science: Part B: Polymer Physics*, 44, 1096-1105, DOI:10.1002/polb.20766.

[81] Yang, H. S., & Park, E. S. (2006). Mechanical properties and antimicrobial activity of silicone rubber compounds containing acrylated norfloxacin and its polymer. *Macromolecular Materials and Engineering*, 291, 621-628.

[82] Yoon, K. R., Kim, W. J., & Choi, I. S. (2004). Functionalization of Shortened Single-Walled Carbon Nanotubes with Poly(p-dioxanone) by "Grafting-From" Approach. *Macromolecular Chemistry and Physics*, 205, 1218-1221.

[83] Yurekli, K., Mitchell, C. A., & Krishnamootri, R. (2004). Small-angle neutron scattering from surfactant-assisted aqueous dispersions of carbon nanotubes. *Journal of the American Chemical Society*, 126, 9902-9903.

[84] Zhao, J. J., Park, H. K., Han, J., & Lu, J. P. (2004). Electronic properties of carbon nanotubes with covalent sidewall functionalization. *J. Phys. Chem. B*, 108, 4227-4230.

[85] Zeleniakiene, D. (2006). The influence of microstructural stiffness changes on the stress concentration factor of porous polymer materials. *Proceedings of the Estonian Academy of Sciences Engineering*, 12(2), 147-155, 1406-0175.

[86] Zhang, M., Atkinson, K. R., & Baughman, R. H. (2004). Multifunctional Carbon Nanotube Yarns by Downsizing an Ancient Technology. *Science*, 306(5700), 1358-1361.

[87] Zhu, L., Xu, J., Xiu, Y., Hess, W. H., & Wong, C. P. (2006). Controlled Growth and Electrical Characterization of High-aspect ratio Carbon Nanotube Arrays. *Carbon*, 4, 253-258.

[88] Zhu, H. W., Xu, C. L., Wu, D. H., Wei, B. Q., Vajtai, R., & Ajayan, P. M. (2002). Direct synthesis of long nanotube strands. *Science*, 296, 884-886.

[89] Zou, J. H., Liu, L. W., Chen, H., Khondaker, S. I., McCullough, R. D., & Huo, Q. (2008). Dispersion of pristine carbon nanotubes using conjugated block copolymers. *Advanced Materials*, 20, 2055-2060, 1521-4095.

IntechOpen